

Dual Inhibition of Pyruvate Dehydrogenase Complex and Respiratory Chain Complex Induces Apoptosis by a Mitochondria-Targeted Fluorescent Organic Arsenical *in vitro* and *in vivo*

Yu-Jiao Liu⁺,^[a] Xiao-Yang Fan⁺,^[a] Dong-Dong Zhang,^[b] Yin-Zheng Xia,^[a] Yan-Jun Hu,^[c] Feng-Lei Jiang,^[a] Fu-Ling Zhou,^{*,[b]} and Yi Liu^{*,[a, c, d]}

Based on the potential therapeutic value in targeting mitochondria and the fluorophore tracing ability, a fluorescent mitochondria-targeted organic arsenical PDT-PAO-F16 was fabricated, which not only visualized the cellular distribution, but also exerted anti-cancer activity *in vitro* and *in vivo* via targeting pyruvate dehydrogenase complex (PDHC) and respiratory chain complexes in mitochondria. In details, PDT-PAO-F16 mainly accumulated into mitochondria within hours and suppressed the activity of PDHC resulting in the inhibition of ATP synthesis

and thermogenesis disorder. Moreover, the suppression of respiratory chain complex I and IV accelerated the mitochondrial dysfunction leading to caspase family-dependent apoptosis. *In vivo*, the acute promyelocytic leukemia was greatly alleviated in the PDT-PAO-F16 treated group in APL mice model. Our results demonstrated the organic arsenical precursor with fluorescence imaging and target-anticancer efficacy is a promising anticancer drug.

Introduction

Arsenical had been used to treat with psoriasis, syphilis or rheumatism in China and Greece since two thousand years ago.^[1] To date the most dramatic finding in the history of arsenical drugs is that arsenic trioxide (ATO) was successfully used to treat acute promyelocytic leukemia (APL)^[2] in 1970 s.^[3] Nowadays, ATO and all-trans retinoic acid (ATRA) have been the first-line treatment regimens to trigger the cell redifferentiation or apoptosis-inducing therapy for APL.^[1c,4] Besides that ATO was approved to treat APL by the Food and Drug Administration (FDA) in 2000,^[5] organic arsenicals darinaparsin (DAR) and 4-(N-(S-glutathionylacetyl)amino) phenylarsonous acid (GSAO) also have been approved by FDA to

carry out the pre-clinical trials for the treatment of cancer, such as leukemia, lymphoma and solid tumor.^[6]

Although many researches focused on the anti-tumor mechanism of ATO in the past several decades,^[7] there are still some problems to be solved. It is widely accepted that ATO can enhance the SUMOylation and ubiquitination leading to the degradation of fusion protein PML-RAR α (expressed by fusion gene of promyelocytic leukemia gene and retinoic acid receptor alpha) and APL cell re-differentiation via the directly binding with the cysteine residues in RBCC (RING-B-box-coiled-coil) domain located in zinc finger motif in PML-RAR α .^[8] However, the research *in vitro* has shown that methylation metabolite MMA^{III} (mono-methyl-arsenic acid) of ATO has the higher affinity toward PML-RAR α fusion protein than that of ATO or other methylation metabolites.^[9] What's more, literature showed that the occurrence of cell re-differentiation may be not dependent on methylated arsenicals.^[9c] These findings indicate the degradation of PML-RAR α fusion protein induced by ATO is a very complicated process. Besides ATO, As₄O₆ and As₄S₄ also demonstrated the better inhibitory ability to many cancer cell lines by various signal pathways.^[10]

Comparing with the inorganic arsenicals, organic arsenicals have some unique advantages including the designable structure, the better biological efficacy and the higher affinity toward the cysteine residues.^[11] Furthermore, organic arsenicals are generally thought to induce the apoptosis rather than cell re-differentiation,^[12] which means organic arsenicals may carry out the anti-cancer efficacy toward leukemia and lymphoma, as well as solid tumors. It has been reported that organic arsenical DAR can induce the cell cycle arrest, mitochondrial dysfunction, MAPK-mediated SHP1-dependent cell death or ROS-mediated apoptosis.^[12b,13] Although the signal pathways activated by DAR are diverse for the different cell lines, the influence on mitochon-

[a] Y.-J. Liu,⁺ X.-Y. Fan,⁺ Y.-Z. Xia, F.-L. Jiang, Prof. Y. Liu
Department of Chemistry
Wuhan University
Wuhan 430072 (China)
E-mail: yiliuchm@whu.edu.cn

[b] Dr. D.-D. Zhang, Prof. F.-L. Zhou
Department of Haematology
Zhongnan Hospital
Wuhan University
Wuhan 430071 (China)
E-mail: zhoufuling@whu.edu.cn

[c] Dr. Y.-J. Hu, Prof. Y. Liu
College of Chemistry and Materials Science
Nanning Normal University
Nanning 530001 (China)

[d] Prof. Y. Liu
School of Chemistry and Chemical Engineering
Wuhan University of Science and Technology
Wuhan 430081 (China)

[⁺] These authors contributed equally to this work.

 Supporting information for this article is available on the WWW under <https://doi.org/10.1002/cmdc.201900686>

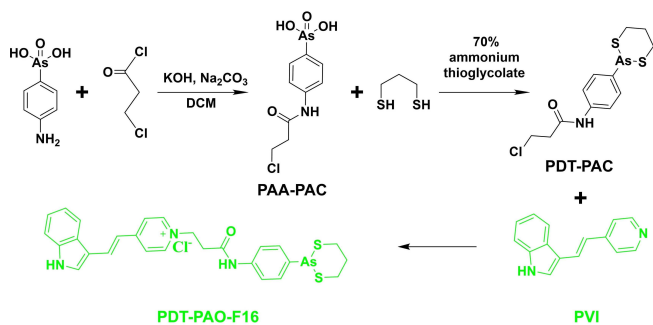
dria is not neglected in all functional mechanisms. Additionally, organic arsenical GSAO inhibiting the neovascularization and cell proliferation is closely related to the reaction between the metabolite CAO of GSAO and adenine nucleotide translocase (ANT) in mitochondria.^[14] Moreover, our former researches also support the viewpoint that mitochondria play the vital role in the cytotoxicity of organic arsenicals and many other drugs.^[15]

Based on these reports, we got a mitochondria-targeted fluorescent organic arsenical to improve the anti-cancer activity and visualize the distribution in the cells at the same time. Supported by the literature that F16, a mitochondria-targeted fluorescent compound, impaired the mitochondrial function to initiate cellular apoptosis or necrosis,^[16] we found that PDT-PAO-F16 mainly accumulated in mitochondria and displayed the better inhibitory efficacy. Surprisingly, PDT-PAO-F16 showed the dual inhibition toward pyruvate dehydrogenase complex (PDHC) and respiratory chain complexes. After the systematic mechanism exploration, the observations revealed that PDT-PAO-F16 triggered the respiration dysfunction, thermogenesis disorder, membrane swelling and enhanced permeability, resulting in the release of cytochrome c and the activation of caspase-dependent ROS-mediated apoptosis. As well, it exhibited good inhibitory ability toward APL in mice model.

Results and Discussion

Synthesis and characterization of PDT-PAO-F16

Similar with ATO associated with mitochondrial dysfunction, more and more reports have shown that organic arsenicals can induce the mitochondria-mediated or ROS-mediated cell death.^[11d,15a] F16 as the cationic form of PVI could accumulate into mitochondria and cause mitochondria dysfunction. Linking the targeting compound F16 with the compound PAO-PDT with highly anticancer efficiency (Scheme 1), we got the targeting compound PDT-PAO-F16. The UV-vis spectrum ranging from 400 nm to 500 nm characterized the PVI moiety and the absorbance near 270 nm belonged to the S–As–S bond (Figure 1A).^[17] In addition, PDT-PAO-F16 showed the maximum excitation at 451 nm and the maximum emission at 555 nm (Figure 1B).



Scheme 1. Synthesis of PDT-PAO-F16 ((*E*)-1-(3-((4-(1,3,2-dithiasinan-2-yl)phenyl)amino)-3-oxopropyl)-4-(2-(1*H*-indol-3-yl)vinyl)pyridin-1-ium).

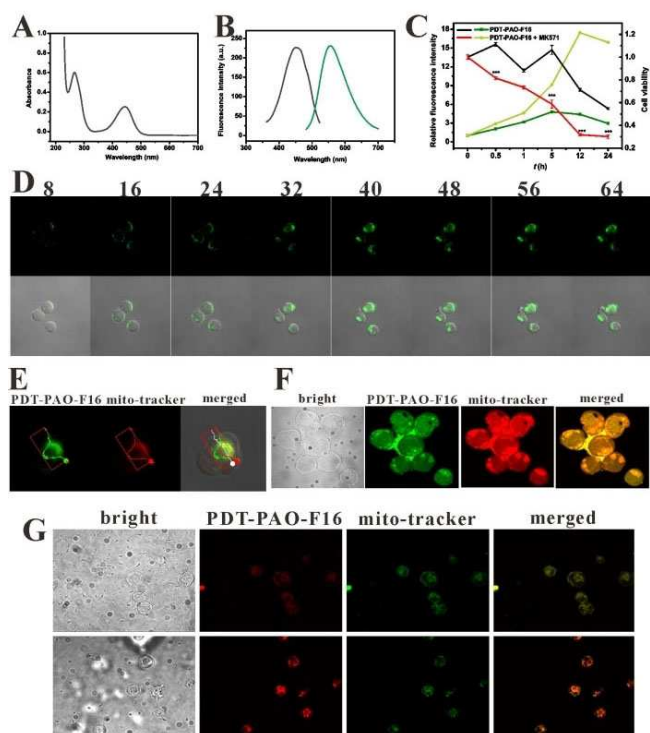


Figure 1. A) and B) Spectra characterization of 10 μM PDT-PAO-F16 in PBS. C) Influence of MK571 on NB4 cellular uptake and cell viability. NB4 cells were incubated with 0.6 μM PDT-PAO-F16 for 0.5 h, 1 h, 5 h, 12 h and 24 h, followed by the flow cytometer assessment and the cell viability assessment. D) Confocal images of PDT-PAO-F16 characterizing its uptake rate. The pictures were snapped 8, 16, 24, 32, 40, 48, 56, 64 min later after 4.8 μM PDT-PAO-F16 was added to the cultural medium of NB4 cells. E) NB4 cells were co-incubated with 4.8 μM PDT-PAO-F16 and 1 μM MitoTracker red for 1 hour and PDT-PAO-F16 and MitoTracker red accumulated at the same position which demonstrated the mito-targeting ability of PDT-PAO-F16. F) NB4 cells were incubated with 1 μM CCCP in advance for 10 min, followed by the addition of 4 μM PDT-PAO-F16 for 3 h and the mitochondrial tracker (MitoTracker[®] Red CM-H₂XRos) staining. G) NB4 cells were incubated with 4.8 μM PDT-PAO-F16 for 3 h, followed by the mitochondrial tracker staining. Upper: 1 μM MitoTracker[®] Red CM-H₂XRos; lower: 1 μM MitoTracker[®] Deep Red FM.

Cellular uptake and mitochondrial accumulation

In order to assess the biological activity, the half-inhibitory concentrations (IC_{50}) of PDT-PAO-F16 for five cancer cell lines (NB4, HL-60, HeLa, MCF-7, SGC7901) were determined by MTT assay. Illustrated in Table S1, PDT-PAO-F16 showed the best efficacy toward leukemia cells among the five cell lines, namely NB4 cells ($IC_{50/24h} = 0.66 \pm 0.14 \mu\text{M}$) and HL-60 cells ($IC_{50/24h} = 0.86 \pm 0.24 \mu\text{M}$). Furthermore, it displayed the toxicity for normal cells (HEK 293 and GES-1) less than that for leukemia cells, which indicated that the introduction of PVI increased the inhibitory capacity, as well as the cellular selectivity. Furthermore, NB4 cells were chose for follow up research.

According to the fluorescent intensity in cells demonstrating the intracellular uptake of PDT-PAO-F16, PDT-PAO-F16 could enter into the NB4 cells and even accumulate in mitochondria within an hour in a time-dependent manner (Figure 1D and 1E) Additionally, pre-treatment of un-coupler CCCP, resulting in the collapse of

mitochondrial membrane potential, induced the random distribution of PDT-PAO-F16, as well as the mitochondrial tracker (Figure 1F). These results demonstrated that PDT-PAO-F16 relied on the mitochondrial membrane potential as a kind of delocalization lipophilic cation (DLC) to mainly target the mitochondria (Figure 1G). Besides, the compound stopped accumulation after the long-time incubation (at least 12 h) (Figure 1C). After the possibility of cell death was ruled out, the most likely reason was that organic arsenical PDT-PAO-F16 was removed from the NB4 cells. The pre-incubation of multi-drug resistance protein 1 (MRP1) inhibitor MK571 could maintain the fluorescence intensity of PDT-PAO-F16 in the NB4 cells even cell death, which indicated the elimination of PDT-PAO-F16 was mediated by the MRP proteins. These results were in accordance with the former researches.^[18] Of course, there may be other possibilities for the compound to be eliminated, such as internal metabolism.

Inhibition of PDHC activity in NB4 cells

The cell viability could be recovered by the incubation together of lipoic acid (LA) (Figure 2A). LA is not only a powerful antioxidant but also a necessary disulfhydryl coenzyme for pyruvate dehydrogenase complex (PDHC). PDHC is a kind of multi-enzyme complex converting pyruvate into acetyl-CoA including pyruvate dehydrogenase (E1), dihydrolipoyltransacetylase (E2) and dihydrolipoamide dehydrogenase (E3) linking the glycolysis metabolic pathway to the citric acid cycle.^[19,20] After cells were incubated together with PDT-PAO-F16, there was a significant decrease in the activity of PDHC in NB4 cells via a dose- and time-dependent manner (Figure 2B). Consider-

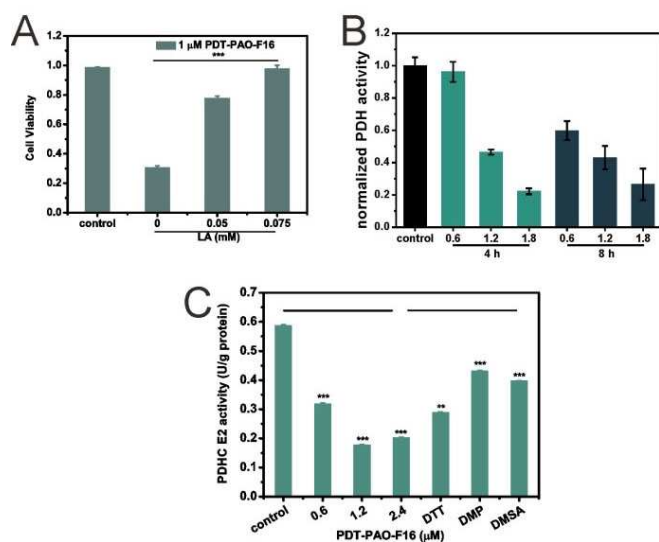


Figure 2. A) The effect of LA on NB4 cell viability with PDT-PAO-F16 incubated for 24 h monitored by trypan blue staining. B) The PDHC activity of NB4 cells. C) The PDHC E2 activity of NB4 cells. NB4 cells with different concentrations of PDT-PAO-F16 were incubated for 3 h or 1.2 μM PDT-PAO-F16 and 500 μM DTT, 300 μM DMP or 100 μM DMSA, then the cells were sacrificed for the PDHC E2 activity assessment by the kit.

ing the high affinity between arsenic and sulfhydryl in LA,^[17,21] it was speculated that PDT-PAO-F16 may affect the E2 activity via perturbing with the sulfhydryl in LA to prevent the acryl group converted to CoA. The observation that the activity of PDHC E2 was suppressed in the presence of PDT-PAO-F16 and recovered to some extent by the co-incubation of dimercapto compounds (DTT (dithiothreitol), DMSA ((*r**,*s**)-2,3-dimercaptobutanedioic acid) and DMP (2,3-dimercapto-1-propanol)) indeed supported the speculation (Figure 2C). Another piece of evidence was obtained that some dimercapto compounds can also protect NB4 cells from death to some extent in spite of the existence of high dosage of PDT-PAO-F16 (Figure S1).

Effect on mitochondrial respiratory chain complexes

The respiratory chain enzyme complexes are responsible for the oxygen consumption and ATP synthesis locating at mitochondria. The addition of PDT-PAO-F16 of low dosage mainly had a remarkable impact on complex I and IV of isolated mitochondria while had negligible impact on complex II and III (Figure 3A). Complex IV is the terminal enzyme complex in electron transport chain, where over 90% of oxygen is consumed, thus it largely controls the mitochondrial respiration.^[22] The mitochondrial respiration of isolated mitochondria and cells was monitored by Clark Oxygen Electrode. Relatively low respiratory rate

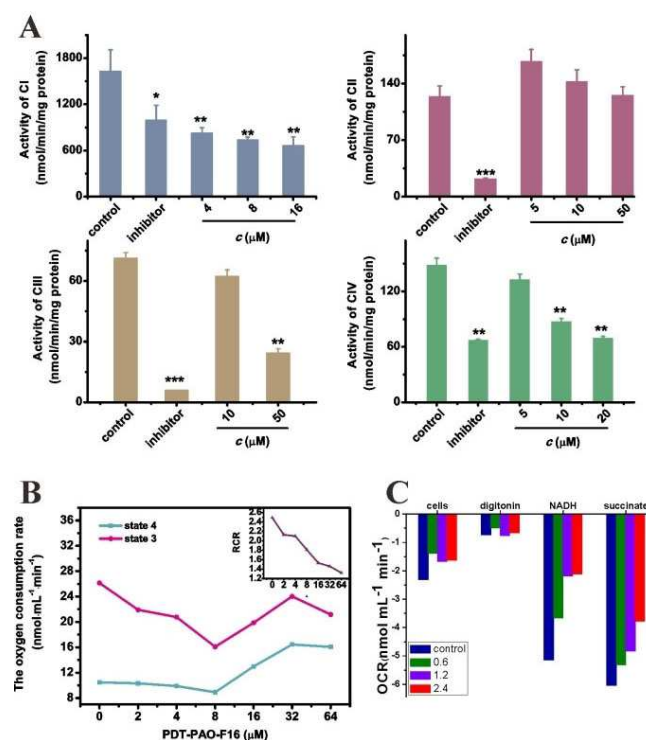


Figure 3. A) The effect on activities of respiratory chain complex I, II, III and IV. B) The effect of mitochondrial respiration in the presence of PDT-PAO-F16. Different concentrations of PDT-PAO-F16 were added into isolated mitochondria. Then the oxygen consumption rate (OCR) of each state was monitored. C) The OCR of NB4 cells under various conditions.

for state 4 characterizes integrate mitochondrial inner membrane and the high respiratory rate for state 3 (about 3-fold higher than state 4) characterizes that respiratory chain functions well. The isolated mitochondria without PDT-PAO-F16 showed low respiratory rate of state 4 and high of state 3 (Figure 3B). After mitochondrial exposure with different concentrations of PDT-PAO-F16, state 4 changed merely until the concentration of PDT-PAO-F16 reached $8\ \mu\text{M}$ while respiratory rate of state 3 decreased a lot until this concentration. They both increased gradually then compared with the $8\ \mu\text{M}$ PDT-PAO-F16 condition. However, both the changes of state 3 and state 4 induced a dramatic decline of respiratory control ratio ($\text{RCR} = \text{state 3}/\text{state 4}$). The effect on respiratory rate demonstrated the inhibition of mitochondrial respiration and the damage of mitochondrial function. As a result, the cellular oxygen consumption rate was decreased after the 24 h incubation of PDT-PAO-F16 (Figure 3C). With the permeabilization of the plasma membrane achieved with $0.1\ \text{mg/mL}$ digitonin to dissipate the respiratory substrates, all the cells came to almost respiratory arrest. And then respiration was initiated with $5\ \text{mM}$ NADH substrate to complex I followed by being provided $5\ \text{mM}$ succinate substrate to complex II. Even with adequate substrate to complex I, cells showed less oxygen consumption in a dosage-dependent manner under PDT-PAO-F16 exposure circumstances. While after the addition of succinate, the oxygen consumption rate decreased in a much slighter tendency, indicating that PDT-PAO-F16 had much more inhibitory impact on complex I than complex II and also impaired other complexes function.

Production of ROS in NB4 cells

It has been pointed out in literature that complex I and III are associated with the generation of ROS.^[23] The disturbance of complex I by PDT-PAO-F16 may lead to the leakage of electrons so as to excessive production of ROS. The influences were dependent on the dose of PDT-PAO-F16 and incubation time (Figure 4A and 4B). The ROS level increased over 2 times even under $0.6\ \mu\text{M}$ PDT-PAO-F16 exposure for 24 h. And under $1.2\ \mu\text{M}$ PDT-PAO-F16 exposure, the accumulated PDT-PAO-F16 within 1 h could cause ROS burst right away and continued to 24 h. During the initial incubation time (3 h to 6 h), there was a temporary drop in intracellular ROS level which may be a result of endogenous antioxidants' elimination, such as glutathione system and thioredoxin system. There were researches pointed that the burst of intracellular ROS can be stimulated by arsenicals, which further makes the oxidative damage to lipids, proteins and DNA in cells.^[24] Besides, as the scavenge reagent for intracellular GSH, the pre-incubation of L-buthionine-(S,R)-sulfoximine (BSO) with NB4 cells decreased the cellular antioxidant capacity, which further resulted the change that cell viability dropped down remarkably even exposed with the nontoxic concentration of PDT-PAO-F16 (Figure S2). This finding also supports the point that the cancer cells with inherently lower levels of GSH are more sensitive to the toxic effects of arsenic.^[25] However, the decline of cell viability can't be

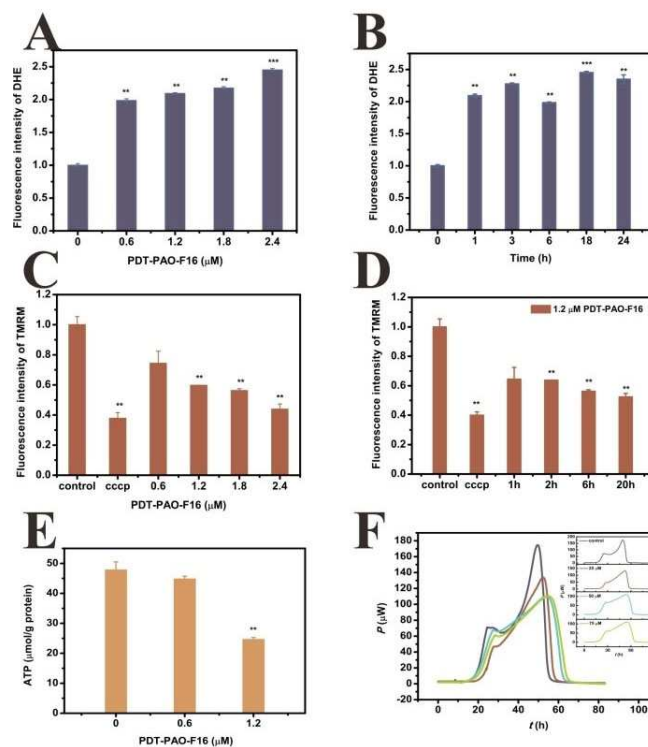


Figure 4. A) and B) The change of intracellular ROS level after exposure for 24 h (A) or with $1.2\ \mu\text{M}$ for different time. C) and D) The collapse of mitochondrial membrane potential of NB4 cells with PDT-PAO-F16. E) The decrease of intracellular ATP level after exposure for 24 h. F) The thermogenic curves of isolated mitochondria taking pyruvate as substrate. After incubated with various concentrations of PDT-PAO-F16, the heat output curves were obtained and analyzed for acquisition of thermogenic parameters.

prevented from PDT-PAO-F16 exposure by some antioxidants, like NAC (N-acetyl-L-cysteine), VC (vitamin C), VE (vitamin E) and so on, which revealed that the burst of ROS was not the initial trigger point by PDT-PAO-F16, but the key step in killing NB4 cells mechanism (data not shown).

Damage on mitochondrial membrane

The accumulation of high level ROS can oxidize DNA, lipids and proteins, especially proteins with some reactive cysteine residues located in vital complexes essential for mitochondrial function.^[26] This indicated that the burst of ROS relied on the disturbance of respiratory chain complexes, as well as connected with the other mitochondrial complexes dysfunction, for instance, the mitochondrial membrane permeability transition pore complex. Under normal circumstances, mitochondrial inner membrane has a low permeability to charged species intrinsically and mitochondrial membrane potential exists.^[27] The isolated mitochondrial membrane permeability to H^+ and K^+ enhanced on PDT-PAO-F16 exposure, evidenced by the decline of absorbance at $540\ \text{nm}$ (Figure S3). Thus it caused the collapse of mitochondrial membrane potential (Figure 4C, 4D

and Figure S4). As well as the permeabilization of membrane, swelling as a result of water influx occurred and the absorbance decreased (Figure S5). Pre-treatment of some specific protective reagents, such as CsA (cyclosporine A), RR (Ruthenium red), EGTA (ethylenbis(oxyethylenitrilo)tetraacetic acid), EDTA ((ethylenediamine)tetraacetic acid), and DTT, could deter the swelling to some extent, which indicated the swelling induced by PDT-PAO-F16 may be the result attributed to concomitance of multiple intricate mechanisms including mitochondrial membrane permeability transition pore opening and the oxidation of active sites in vital proteins.^[28]

Mitochondria play the vital role on supplying metabolic energy to the cell in the form of ATP via direct participating in a number of metabolic reactions, as well as regulating the signal transmission during the apoptosis of cancer cells.^[29] After the mitochondrial damages occurred, the cellular ATP synthesis was interrupted (Figure 4E) and the isolated mitochondrial thermogenesis was interfered monitored (Figure 4F) by microcalorimeter which indicated the impairment of intracellular "energy factory". The relative parameters are concluded in Table S2 and Figure S6.

Induction of caspase family-dependent intrinsic apoptosis

When the outer membrane is ruptured and inner membrane is damaged, some pro-apoptosis proteins could be released into cytoplasm, such as cytochrome *c*, pro-caspases and AIF. Indeed, the content of released cytochrome *c* increased by a dose-dependent way (Figure 5A). The release of cytochrome *c*

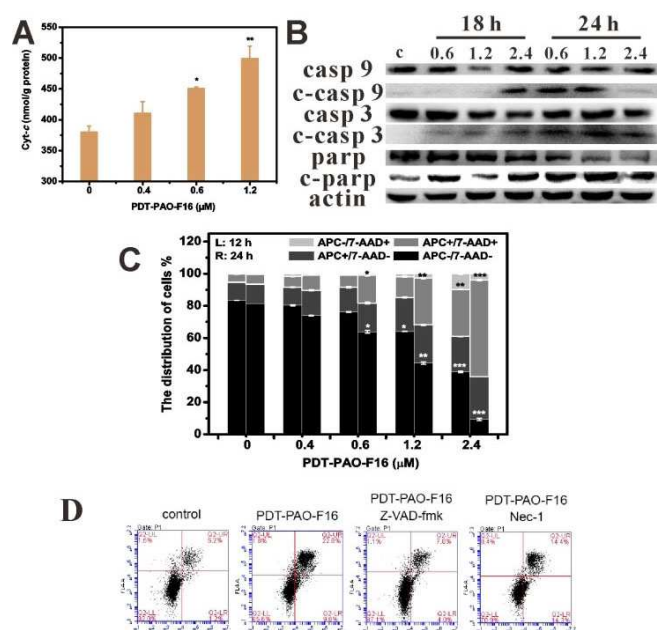


Figure 5. The apoptosis caused by PDT-PAO-F16. A) The increase of intracellular Cyt-*c* level of NB4 cells after incubation for 24 h. B) The expression of some apoptotic signal pathway related proteins. C) Annexin V-APC/7-AAD staining for NB4 cells apoptosis induced by PDT-PAO-F16. D) The effect of Z-VAD-fmk or Nec-1 on apoptosis.

can activate the downstream signals like caspase family leading to cell apoptosis. The content of caspase 9 and caspase 3 decreased with the increase of active cleaved-caspase 9 and cleaved caspase 3 (Figure 5B). And then the cells suffered from DNA damage indicated by the more and more conversion of Parp to cleaved-Parp. At last, it was found that PDT-PAO-F16 induced cellular apoptosis monitored by the Annexin V-APC and 7-AAD double staining via a dose- and time-dependent manner (Figure 5C), which was consistent with the reports that the bulk of arsenicals can activate the apoptotic signaling pathway in many kinds of cell lines.^[12,15a] Besides, the addition of pan-caspase inhibitor Z-VAD-fmk in advance protected the majority of cells from apoptosis, which further confirmed the caspase family-dependent cell apoptosis induced by PDT-PAO-F16 (Figure 5D and Figure S7). Moreover, cellular morphology changed including nuclear shrinkage, chromatin condensation, and apoptotic body formation in the occurrence of apoptosis manifested by Hoechst 33342 and PI staining (Figure S8).

Reducing leukemic burden and inducing long-term survival in an APL mouse model

We further evaluated the PDT-PAO-F16's efficacy in vivo using a transplantable APL mouse model (Figure 6A). C1498 cells, lymphoblast from a female C57BL/6 mouse with acute myeloid

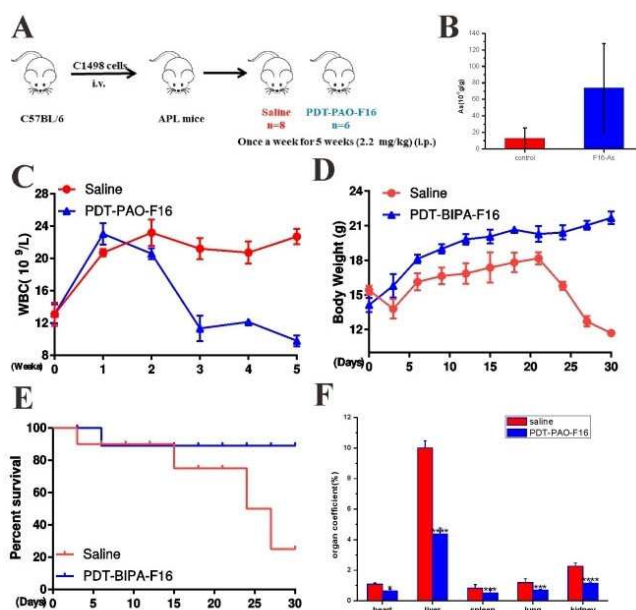


Figure 6. PDT-PAO-F16 reduces leukemia burden in an APL mouse model. A) Schematic representation of transplantable APL mouse model and treatment procedure. B) The arsenic content of mice femur. C) White blood cells counting of the mouse blood before being sacrificed showed reduced leukemic cells in the blood of APL mice. D) The body weight curve of the mice recorded every three days. E) The survival curve shows that PDT-PAO-F16 significantly prolonged the survival compared with the saline group. F) After the mice being sacrificed, the organs were collected and the organ coefficients were calculated according to the organ weight and the related body weight.

leukemia, were injected intravenously via the tail vein into C57BL/6 mice. After the WBC blast, 200 μ L PBS with 2.2 mg/kg PDT-PAO-F16 or not were given intraperitoneally once a week and continued for 5 weeks. Mouse body weight was measured every 3 days. As shown in Figure 6C, PDT-PAO-F16 could alleviate the mice leukemic phenotypes by eliminating abnormal APL cells remarkably compared with the saline group even after the first treatment. Notably, PDT-PAO-F16 could always maintain the body weight increase while the saline group suffered from abnormal body weight loss (Figure 6D) and as a result, our compound prolonged the overall survival of APL mice (Figure 6E). After the mice were sacrificed, the relative organ coefficients demonstrated the transplanted APL cells caused great damage to the mice organ but our compound greatly alleviated or even eliminated the damage (Figure 6F). Besides, the arsenical could accumulate a little in mice femur to withstand the myeloid invasion of leukemic cells without cytotoxicity as the arsenic concentration in femur increased slightly (Figure 6B). Of note: we found the treated group mice were in good health condition during the 5-week treatment period and no signs of toxicity. All these results indicated that PDT-PAO-F16 was a potential candidate for APL.

Conclusion

In conclusion, the newly synthesized organic arsenical PDT-PAO-F16 visualized the cellular distribution, and exerted anti-cancer activity via targeting PDHC and respiratory chain complexes in mitochondria. The introduction of PVI moiety to PDT-PAO-F16 improves anti-cancer activity and selectivity attributed to accumulating in mitochondria in cancer cells as a kind of delocalization lipophilic cation. It mainly inhibited the activity of PDHC and respiratory chain complex I and IV leading to the mitochondrial dysfunction, causing mitochondrial depolarization, ROS generation, suppression of ATP synthesis and thermogenesis disorder. Thus it led to the release of cytochrome *c* and caspase family-dependent cell apoptosis. Importantly, it could inhibit leukemic cell blast in APL mice and showed almost no side effect. To sum up, this study provides insights into the design and the anti-cancer mechanism of organic arsenical and also provides a promising viable therapy for APL.

Experimental Section

Experimental details and supporting results are available in the Supporting Information.

Acknowledgements

We gratefully acknowledge financial support from the National Natural Science Foundation of China (21673166, 21873075), and the Fundamental Research Funds for the Central Universities (2015203020212). We thank Fang Zhou for providing confocal services (Analytical & Testing Center, IHB, CAS).

Keywords: Arsenic · leukemia · mitochondria · PDHC · apoptosis

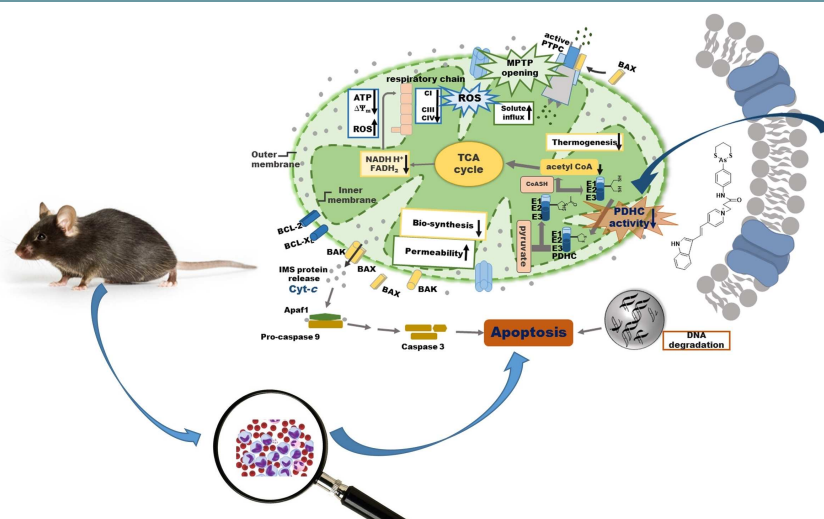
- [1] a) S. Waxman, K. C. Anderson, *Oncologist* **2001**, *6*, 3–10; b) S. Gibaud, G. Jaouen, in *Medicinal organometallic chemistry*, Springer, **2010**, 1–20; c) J. Zhu, Z. Chen, V. Lallemand-Breitenbach, *Nat. Rev. Cancer* **2002**, *2*, 705–714.
- [2] C. Huynh, D. Roth, D. M. Ward, J. Kaplan, N. W. Andrews, *Proc. Natl. Acad. Sci. USA* **2004**, *101*.
- [3] M. A. Sanz, P. Fenaux, M. S. Tallman, E. H. Estey, B. Löwenberg, T. Naoe, E. Lengfelder, H. Döhner, A. K. Burnett, S.-J. Chen, V. Mathews, H. Iland, E. Rego, H. Kantarjian, L. Adès, G. Avvisati, P. Montesinos, U. Platzbecker, F. Ravandi, N. H. Russell, F. Lo-Coco, *Blood* **2019**, *133*, 1630.
- [4] F. Massaro, M. Molica, M. Breccia, *Int J Hematol Oncol* **2016**, *5*, 105–118.
- [5] B. R. Smith, C. M. Eastman, J. T. Njardarson, *J. Med. Chem.* **2014**, *57*, 9764–9773.
- [6] a) P. C. Lloyd, H. W. Morgan, B. K. Nicholson, R. S. Ronimus, *Angew. Chem. Int. Ed.* **2005**, *44*, 941–944; *Angew. Chem.* **2005**, *117*, 963–966; b) B. K. Mandal, Y. Ogra, K. T. Suzuki, *Chem. Res. Toxicol.* **2001**, *14*, 371–378.
- [7] a) P. J. Dilda, P. J. Hogg, *Cancer Treat. Rev.* **2007**, *33*, 542–564; b) V. Lallemand-Breitenbach, J. Zhu, Z. Chen, *Trends Mol. Med.* **2012**, *18*, 36–42.
- [8] X.-W. Zhang, X.-J. Yan, Z.-R. Zhou, F.-F. Yang, Z.-Y. Wu, H.-B. Sun, W.-X. Liang, A.-X. Song, V. Lallemand-Breitenbach, M. Jeanne, *Science* **2010**, *328*, 240–243.
- [9] a) H. Naranmandura, N. Suzuki, K. T. Suzuki, *Chem. Res. Toxicol.* **2006**, *19*, 1010–1018; b) K. T. Suzuki, A. Katagiri, Y. Sakuma, Y. Ogra, M. Ohmichi, *Toxicol. Appl. Pharmacol.* **2004**, *198*, 336–344; c) Q. Q. Wang, X. Y. Zhou, Y. F. Zhang, N. Bu, J. Zhou, F. L. Cao, H. Naranmandura, *Oncotarget* **2015**, *6*, 25646.
- [10] a) M. J. Kim, J. H. Jung, W. S. Lee, J. W. Yun, J. N. Lu, S. M. Yi, H. J. Kim, S.-H. Chang, G.-S. Kim, S. C. Hong, *Oncol. Rep.* **2014**, *31*, 2305–2311; b) L. Zhang, Y. Tong, X. Zhang, M. Pan, S. Chen, *Drug Des. Dev. Ther.* **2015**, *9*, 5851.
- [11] a) S. Shen, X.-F. Li, W. R. Cullen, M. Weinfeld, X. C. Le, *Chem. Rev.* **2013**, *113*, 7769–7792; b) M. J. Mass, A. Tennant, B. C. Roop, W. R. Cullen, M. Styblo, D. J. Thomas, A. D. Kligerman, *Chem. Res. Toxicol.* **2001**, *14*, 355–361; c) E. Dopp, U. Von Recklinghausen, R. Diaz-Bone, A. Hirner, A. Rettenmeier, *Environ. Res.* **2010**, *110*, 435–442; d) Y. Liu, D. Duan, J. Yao, B. Zhang, S. Peng, H. Ma, Y. Song, J. Fang, *J. Med. Chem.* **2014**, *57*, 5203–5211.
- [12] a) G.-Q. Chen, L. Zhou, M. Styblo, F. Walton, Y. Jing, R. Weinberg, Z. Chen, S. Waxman, *Cancer Res.* **2003**, *63*, 1853–1859; b) I. Khairul, Q. Q. Wang, Y. H. Jiang, C. Wang, H. Naranmandura, *Oncotarget* **2017**, *8*, 23905.
- [13] a) D. Ravi, S. Bhalla, R. B. Gartenhaus, J. Crombie, J. Sharma, I. K. Kandela, A. P. Mazar, A. M. Evens, *Clin. Cancer Res.* **2014**, *15*, 1532; b) A. S. Don, O. Kisker, P. Dilda, N. Donoghue, X. Zhao, S. Decollogne, B. Creighton, E. Flynn, J. Folkman, P. J. Hogg, *Cancer Cell* **2003**, *3*, 497–509.
- [14] a) D. Park, J. Chiu, G. G. Perrone, P. J. Dilda, P. J. Hogg, *Cancer Cell Int.* **2012**, *12*, 11; b) M. Elliott, S. Ford, E. Prasad, L. Dick, H. Farmer, P. Hogg, G. Halbert, *Int. J. Pharm.* **2012**, *426*, 67–75.
- [15] a) X.-Y. Fan, X.-Y. Chen, Y.-J. Liu, H.-M. Zhong, F.-L. Jiang, Y. Liu, *Sci. Rep.* **2016**, *6*; b) M. Picard, D. C. Wallace, Y. Burelle, *Mitochondrion* **2016**, *30*, 105–116; c) M. Vuda, A. Kamath, *Mitochondrion* **2016**, *31*, 63–74.
- [16] V. R. Fantin, P. Leder, *Cancer Res.* **2004**, *64*, 329–336.
- [17] A. M. Spuches, H. G. Kruszyna, A. M. Rich, D. E. Wilcox, *Inorg. Chem.* **2005**, *44*, 2964–2972.
- [18] a) L. D. Garbinski, B. P. Rosen, J. Chen, *Environ. Int.* **2019**, *126*, 585–597; b) S. Xu, Y. F. Zhang, M. W. Carew, W. H. Hao, J. F. C. Loo, H. Naranmandura, X. Chris Le, *Arch. Toxicol.* **2013**, *87*, 1013–1023.
- [19] E. L. Guevara, N. S. Nemerita, L. Yang, F. Jordan, *FASEB J.* **2016**, *30*, 851–856.
- [20] E. Saunier, C. Benelli, S. Bortoli, *Int. J. Cancer* **2016**, *138*, 809–817.
- [21] a) X. Yan, J. Li, Q. Liu, H. Peng, A. Popowich, Z. Wang, X. F. Li, X. C. Le, *Angew. Chem. Int. Ed.* **2016**, *55*, 14051–14056; *Angew. Chem.* **2016**, *128*, 14257–14262; b) Z. Diaz, K. K. Mann, S. Marcoux, M. Kourelis, M. Colombo, P. B. Komarnitsky, W. H. Miller, Jr., *Leukemia* **2008**, *22*, 1853–1863.
- [22] A. Birk, W. Chao, C. Bracken, J. Warren, H. Szeto, *Br. J. Pharmacol.* **2014**, *171*, 2017–2028.
- [23] M. P. Murphy, *Biochem. J.* **2009**, *417*, 1–13.

- [24] B. Halliwell, *Trends Pharmacol. Sci.* **2011**, *32*, 125–130.
 [25] C.-H. Yang, M. Kuo, J. Chen, Y. Chen, *Brit. J. cancer* **1999**, *81*, 796.
 [26] P. R. Angelova, A. Y. Abramov, *Free Radical Biol. Med.* **2016**, *100*, 81–85.
 [27] G. Kroemer, L. Galluzzi, C. Brenner, *Physiol. Rev.* **2007**, *87*, 99–163.
 [28] a) T.-I. Peng, M.-J. Jou, *Ann. N. Y. Acad. Sci.* **2004**, *1011*, 112–122; b) M. González-Durruthy, J. M. Monserrat, L. C. Alberici, Z. Naal, C. Curti, H. González-Díaz, *RSC Adv.* **2015**, *5*, 103229–103245.
 [29] a) A. J. Kastaniotis, K. J. Autio, J. M. Kerätär, G. Monteuuis, A. M. Mäkelä, R. R. Nair, L. P. Pietikäinen, A. Shvetsova, Z. Chen, J. K. Hiltunen, *BBA-Mol.*

Cell Biol. L. **2017**, *1862*, 39–48; b) S. Desagher, J.-C. Martinou, *Trends Cell Biol.* **2000**, *10*, 369–377.

Manuscript received: December 7, 2019
 Revised manuscript received: February 10, 2020
 Version of record online: ■■■, ■■■■

FULL PAPERS



Y.-J. Liu, X.-Y. Fan, Dr. D.-D. Zhang,
Y.-Z. Xia, Dr. Y.-J. Hu, F.-L. Jiang,
Prof. F.-L. Zhou*, Prof. Y. Liu*

1 – 8

Dual Inhibition of Pyruvate Dehydrogenase Complex and Respiratory Chain Complex Induces Apoptosis by a Mitochondria-Targeted Fluorescent Organic Arsenical in vitro and in vivo

A fluorescent mitochondria-targeted organic arsenical PDT-PAO-F16 was fabricated, and was found to accumulate in mitochondria within hours and to inhibit the activity of PDHC and respiratory chain complex I and IV, leading to mitochondrial dysfunction.

This further caused caspase-family-dependent cell apoptosis in vitro and in vivo. Owing to this apoptotic-inducing ability, PDT-PAO-F16 alleviated and even diminished acute promyelocytic leukemia cells in mice.